JME

Journal of Mining & Environment,
Vol. 9, No. 3, 2018, 667-677.
DOI: 10.22044/jme.2018.6783.1501

Estimation of coal seams gas content for evaluating potential use of methane drainage system in Tabas coal mine

M. Mohtasham Seyfi[1], J. Khademi Hamidi[1*], M. Monjezi[1] and A. Hosseini[2]

1. Department of Mining Engineering, Faculty of Engineering & Technology, Tarbiat Modares University, Tehran, Iran
2. Research & Training Department, Tabas Parvadeh Coal Company (TPCCO), Tabas, Iran

Received 12 February 2018; received in revised form 18 March 2018; accepted 18 March 2018
**Corresponding author: jafarkhademi@modares.ac.ir (J. Khademi Hamidi).*

Abstract

Methane gas emission, accumulation, and explosion are the most important risk factors in underground coal mines. Hence, having a knowledge of methane gas emission potential in underground coal mines is of crucial importance in preventing the explosion risk, loss of life, and property, and providing miners' safety. The purpose of this work is to provide the prediction maps for the C_1, C_2, and B_2 coal seams gas contents, and to identify high gas content panels in the Parvadeh No. 1, Tabas coal mine. For this, the data collected from exploratory boreholes is put into geostatistical analysis in ArcGIS in order to estimate the coal seams gas content in unsampled points using the kriging estimation method. Reviewing the gas content maps has revealed that seams of C_1, B_2, and C_2 have gas contents more than 15 cubic meters per ton in about 84%, 55%, and 22% of the understudied area, respectively. The present work highlights the potential and the need for implementation of a methane pre-drainage system, particularly in deeper longwall panels.

Keywords: *Gas Content, Geographic Information System, Geostatistics, Prediction Map.*

1. Introduction

Since 1700's, coal mining has started in deeper depths in the United Kingdom, and catastrophic methane explosions have occurred [1]. A review of the statistics of global coal production shows that a majority of accidents with fatal outcomes are caused by methane gas explosions [2]. Coal seam gas represents a potentially significant risk to the safety and productivity of coal mining operations. The explosion of methane gas in coal mines in many cases has caused loss of life and property worldwide. For example, in the two years to December 2010, more than 561 lives were lost in coal mines as a direct result of methane gas explosions and outbursts [3].

Therefore, awareness on the amount of gas content in coal seams before starting mining operations has a significant effect on preventing the loss of life and property.

Despite the potential dangers of mining operations, coal has many important uses, primarily as a fuel and a source of energy in electricity generation, steel production, and cement manufacturing. Also a closer look into the future trends in coal mining indicates that the conventional use of coal will continue at least until the end of this century [4] but the alternative use of coal such as coal-bed methane (CBM) production will become a common practice, especially from seams that are small, narrow, deep or near populated areas [5]. CBM is categorized as unconventional hydrocarbon, which is produced from coal seams. Research works on CBM have started since a few decades ago, particularly in the United States.

Taking into consideration the important role of methane gas in mining danger, environmental issues, and energy production, particularly in the recent years, extended studies have been conducted on the mechanism of emission of methane gas in coal seams, and identifying the factors influencing and predicting the gas emission rates. For instance, Karacan [6] has presented a supervised artificial neural network (ANN)-based CBM prediction model using a database consisting of the ventilation emission data obtained from 63 US longwall mines for ten years. The author has reported that there are various geological and operational factors including gas content, coal rank, depth of coal seam, panel dimension, cut depth, face conveyer and stage loader speed, and coal production, and a number of entries influencing the methane gas emission in coal mines. Also Karacan et al. [7] have employed the sequential Gaussian simulation for geostatistical modeling of the gas emission zone and gas content in Pittsburgh seam mines. Also with a preliminary study on the gas storage capacity and gas-in-place for CBM potential in Balingian coalfield (Sarawak, Malaysia), Chen et al. [8] have reported that the integration of gas content data with geological and operational data is a suitable method available to estimate the methane gas emission in coal mines, and choosing the necessary ventilation equipment. Lv et al. [9] have investigated the impacts of the dominant factors including the burial depth and thickness of the coal, gas content, porosity and permeability, fracturing effect, and hydrogeological conditions on CBM well production in high-rank coalbed methane fields using a bivariate correlation analysis and gray system theory. By utilizing the quantification theory, Hu et al. [10] have investigated the correlation between the methane content and the influential factors such as depth of coal seam, porosity, volatile material, moisture percentage, and coal ash. Fu et al. [11] have reported that the methane gas content increases with increase in the coalbed burial depth. They have also found that during the same conditions of burial depth, roof sealing, and gas content, the thicker the coal seam is, the higher the CBM resource potential is. Sarhosis et al. [12] have studied the economic modelling of coal bed methane production and electricity generation from deep virgin coal seams. They have concluded that the permeability of coal seam is one of the most effective factors directly related to the methane gas production rate. More recently, Sereshki et al. [13] have evaluated the effect of macerals on coal seam permeability. Also in a laboratory scale study carried out on the specimens taken from Tabas and Shahrood coal mines, Taheri et al. [14] have measured the impact of coal macerals on the level of methane gas emission. They have found that there is a relationship between the compositions of maceral in a coal specimen and its permeability level. Ghanbari et al. [15] have determined coal bed methane potential using rock engineering systems in Eastern Alborz coal mines.

The purpose of this work was to estimate the seam gas content of Tabas mine coal as a preliminary study to evaluate the potential use of methane drainage system using the geostatistical analysis in the geographical information system (GIS) environment. Within coal mining, GIS has been used mainly for risk assessment, safety purposes, and CBM production potential evaluation. For instance, Prakash and Vekerdy [16] have employed GIS and remote sensing in order to develop a coal fire monitoring and management information system named CoalMan, and have implemented the system in North China coal mines. Johnson et al. [17] have proposed a GIS-based method for modeling regional hydrogen infrastructure deployment using detailed spatial data, and applied the method to a case study of a potential coal-based hydrogen transportation system in Ohio with CO_2 capture and storage (CCS). Şalap et al. [18] have developed a GIS-based monitoring and management system for underground coal mining safety in three levels as constructive safety, surveillance and maintenance, and emergency. In the work conducted by Yao et al. [19], the potential for CBM production from the Weibei coalfield (Chine) was evaluated based on the GIS-based AHP model together with evaluating the parameters including coal thickness, gas content, coal rank, CBM resource concentration, permeability, porosity, burial depth, and tectonic type. Sutcu [20] has employed GIS to discover the potential coalfields in a region in Turkey taking into account the formation, geologic age, lithology, rock types, depositional environment, distance to fault, and slope data of the studied area as variables.

More recently, Vaziri et al. [21] have used geostatistical analysis in the ArcGIS environment to estimate the coal gas content, and build a gas map for the C_1 seam of Tabas coal mine. The gas content prediction map was then combined with prediction maps of Coal Mine Roof Rating (CMRR), initial in-situ stress state, fault throw, and orientation in an integrated GIS-based model for the purpose of geohazard risk assessment [22]. This model was extended in the present work to evaluate the gas content of three coal seams, and its variation and relation with seam depth in Tabas coal mine. A literature survey has revealed that the gas content is one of the most important parameters influencing the gas emission in underground coal mines. On the other hand, the impact of adjacent seams on gas emission rate in a multi-seam coal basin has been the research subject of few studies in the literature. Hence, the look into the gas content of three coal seams will help find a pass way for the potential use of the gas drainage technique to be used for the next deeper panels.

2. Methodology

In the present work, the gas contents of three coal seams in Tabas coal mine, Parvadeh#1, including C_1, C_2, and B_2 was estimated using the exploratory borehole data. For this purpose, a database consisting of data from 30 exploratory boreholes was developed. The coal seam gas contents in unsampled points were estimated using the kriging interpolation method in the Arc GIS environment. Finally, a zonation of gas contents of coal seams throughout the whole understudied area was presented. Figure 1 shows the methodology and research steps followed in this work. The present work made it possible to estimate the coal seam gas content prior to coal mining operations.

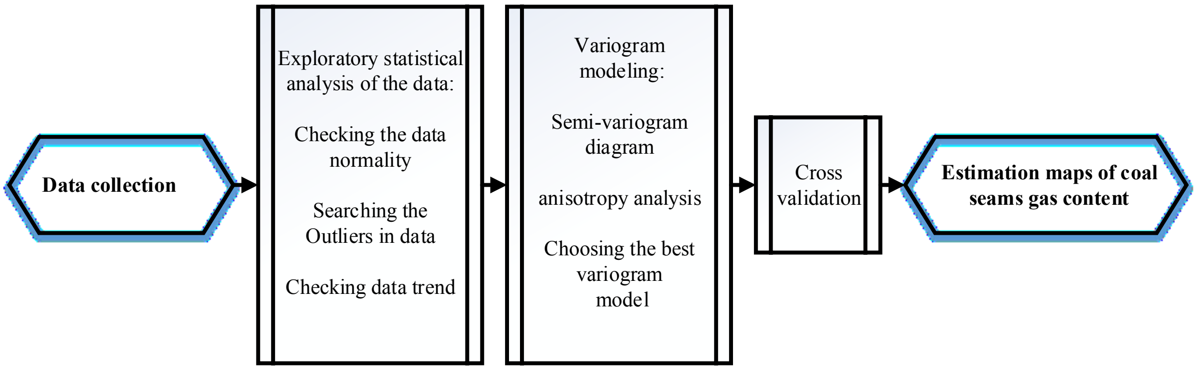

Figure 1. Steps for estimating gas contents of three coal seams in Tabas coal mine.

3. Tabas coal mine

Parvadeh underground coal mine is situated approximately 85 km SE of the city of Tabas in the Southern Khorasan province in Iran. The coal reservoir was estimated to be about 98 Mt. The Parvadeh basin includes five coal seams, namely C_1, C_2, B_1, B_2, and D. Currently, C_1 is under extraction using a mechanized longwall system. The Tabas coal basin stratigraphic column is illustrated in Figure 2. The average thickness, gas content, and geological reserve for each coal seam are given in Table 1.

To the date of the present study, the panels E_1, E_2, W_1, W_0, and W_2 (of 27 designed panels) were extracted. Currently, the E_0 panel with the specifications given in Table 2 is under extraction. The geographical location of the Tabas coal mine along with the layout of nine panels within the studied area is shown in Figure 3.

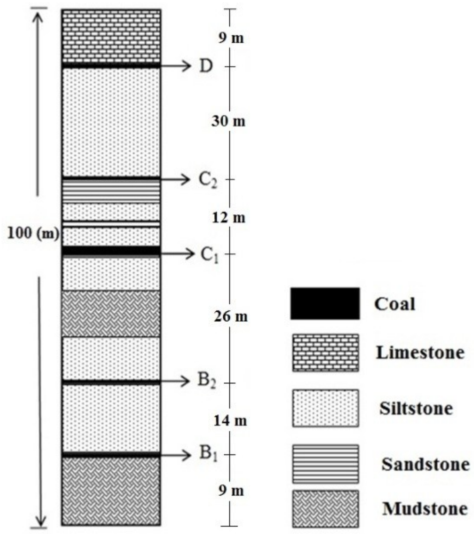

Figure 2. Tabas coal basin stratigraphic column (after Vaziri et al. [22]).

Table 1. Average thickness, gas content, and geological reserve of Parvadeh coal seams.

Parameter \ Coal seam	D	C_2	C_1	B_2	B_1
Average thickness (m)	0.6	0.52	1.83	0.87	0.99
Geological reserves (ton)	5824000	4696000	37469000	7342000	20873000
Gas content (m^3/ton)	8.64	12.42	17.06	12.07	13.04

Table 2. Specifications of panel E_0 in Tabas coal mine.

Parameter	Width (m)	Length (m)	Cutting depth (m)	Cutting height (m)	Panel depth (m)	Dip angle (deg)	Methane recorded in exhaust air (%)
Value	205	1150	0.8	1.9	150	18	1.02

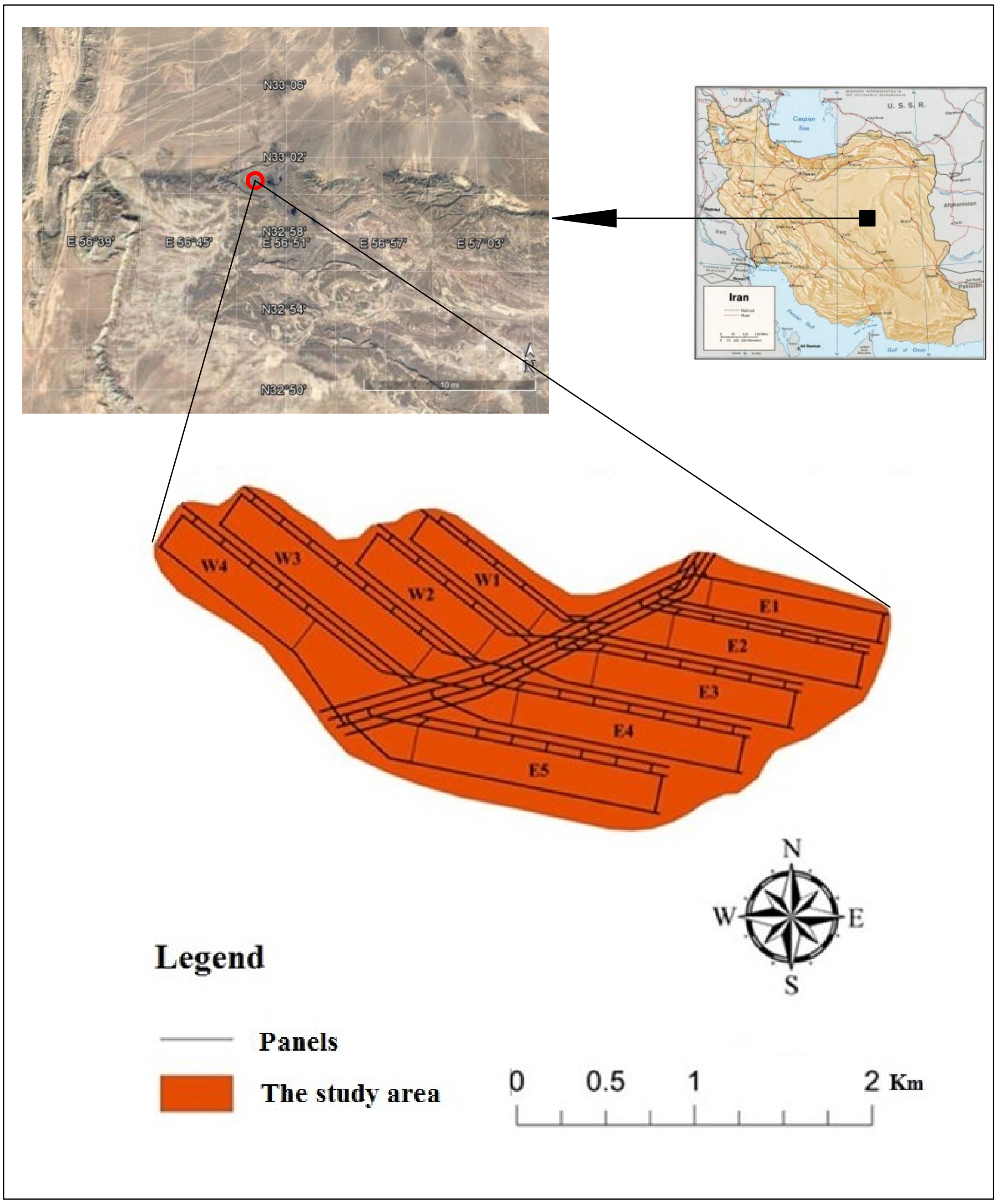

Figure 3. Geographical location of Tabas coal mine and panel layouts in understudied area.

4. Estimation of coal seam gas contents

The gas content data gathered during the exploration drilling program was used to develop a database. A summary of the descriptive statistics for the database is given in Table 3.

Table 3. Descriptive statistics of coal seam gas content data.

Parameter \ Coal seam	B_2	C_2	C_1
Minimum	1.06	4.1	11
Maximum	20.87	17.52	22
Average	12.07	12.42	17.06
Median	13	13.4	17.6
Standard deviation	5.787	3.96	2.53
Skewness	-0.35	-0.64	-0.5
Kurtosis	2.17	2.777	2.88

In order to estimate the gas contents in unsampled areas, the kriging interpolation technique was used. The general equation of kriging estimator is as follows [23]:

$$Z^{*}(x_i) = \sum_{i=1}^{n} l_i Z(x_i) \quad (1)$$

where $Z^{*}(x_i)$ is the estimated value in the x_i point, l_i is the ith sample weight, and $Z(x_i)$ and n represent the measured value of the i^{th} sample and the number of samples, respectively.

Kriging fits a mathematical function to a specified number of points or all points within a specified radius in order to determine the output value for each location. It is a multi-step process including exploratory statistical analysis of the data, variogram modeling, and creating the surface [24].

4.1. Data processing

In this work, the gas content data of the three coal seams were processed before selecting and fitting the most appropriate variogram model. This includes the analyses given in step two in Figure 1 (i.e. checking data normality, outlier analysis, and trend analysis). Interpolation techniques are dependent on data distribution, and provide the best results when the data follows a normal distribution [25]. In this work, the distribution of coal seam gas content data was checked using a histogram tool, as illustrated in Figure 4. As seen, the gas content data for the three coal seams follows a normal distribution. If the data is highly skewed, then linear, box-cox or logarithmic techniques are usually utilized to make the data normal [26].

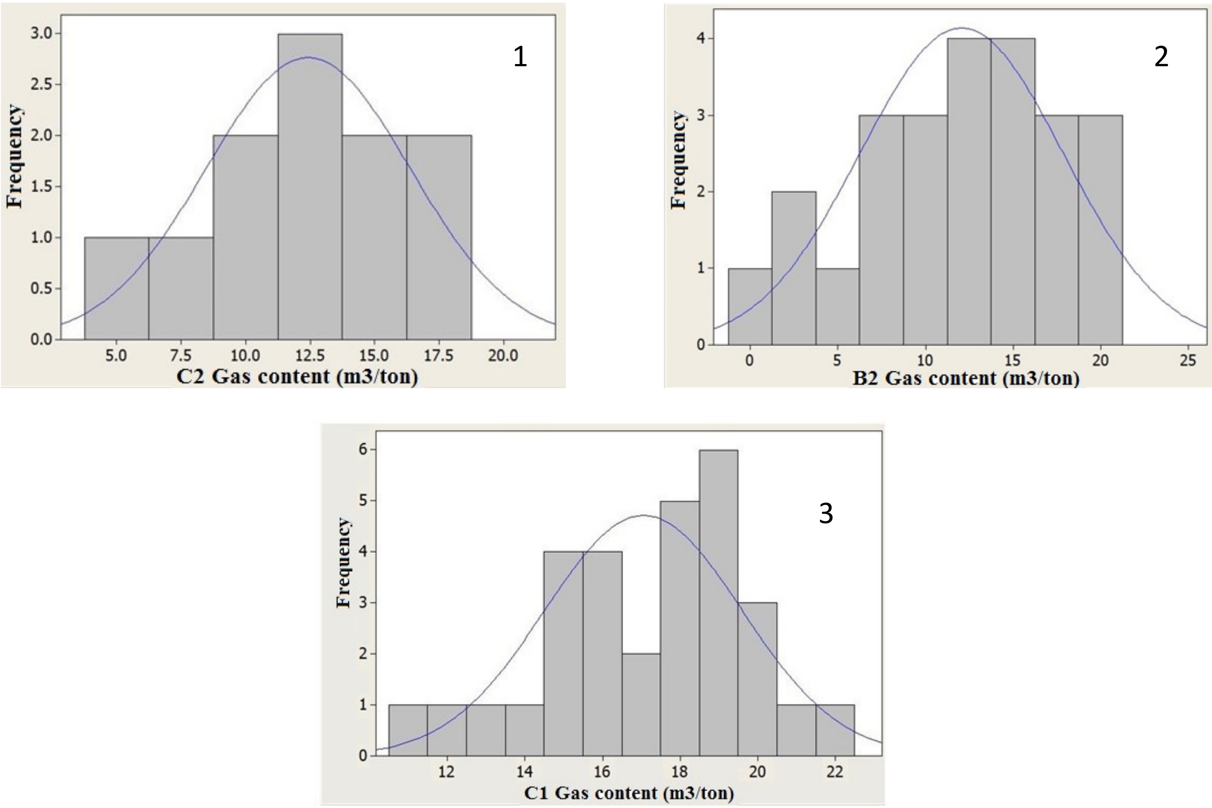

Figure 4. Histogram of gas content data for coal seams 1) C_2, 2) B_2, and 3) C_1.

Next, the outlier analysis was conducted to check the presence of the local and global errors in the coal seam gas content data. The semi-variogram cloud plot illustrating the semi-variance between paired data values against their distance is shown for the three coal seams in Figure 5. As seen, there are neither global nor local outliers in the three coal seam gas content data.

The next step is to perform a trend analysis on the data to check the presence of global trend, which may arise due to topography. Trend, if present, should be removed so that the data could meet the condition of stationarity, which is necessary for using kriging as an interpolation technique. Existence of trend in the data was evaluated using the Trend analysis tool in ArcGIS, as typically illustrated for the gas content data of C_1 coal seam in Figure 6. As it can be followed in the figure, trend is seen in both the NS and EW directions. In order to eliminate the effect of trend on the following geostatistical analysis, the trend of data was removed.

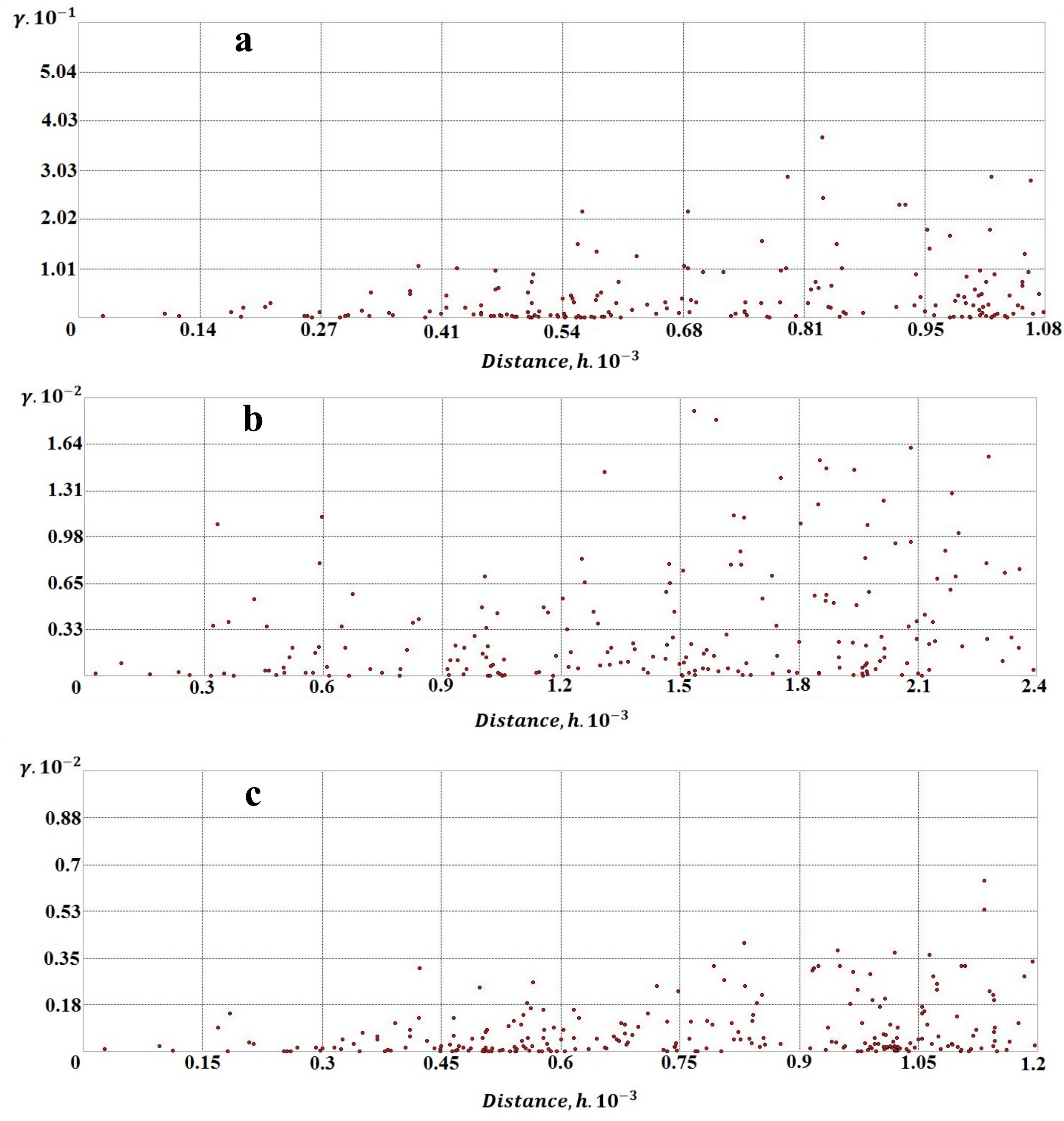

Figure 5. Outlier analysis of gas content data for coal seams: a) C_1, b) B_2, and c) C_2.

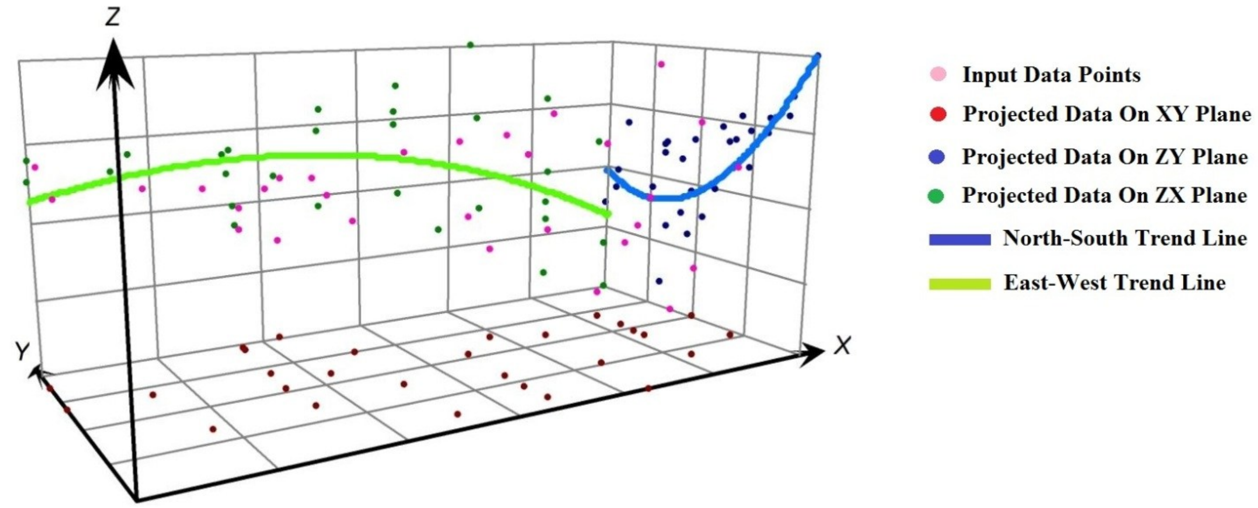

Figure 6. Trend analysis in C_1 coal seam gas content data.

4.2. Variography

Semi-variogram is a geostatistical tool available for measuring the spatial correlation of a regional variable. The general equation of the semi-variogram is as follows [27]:

$$\gamma(h) = \frac{1}{2(n(h))} \sum_{i=1}^{n(h)} (z(x_i + h) - z(x_i))^2 \qquad (2)$$

where $\gamma(h)$ is the semi-variogram value, $n(h)$ is the number of sample pairs that are in the h distance from each other, and $z(x_i)$ is the value of the variable at point x_i.

To actually account for the directional influences on the semi-variogram model, the directional search tool was used, and the anisotropic semi-variogram model was developed. In this research work, variography was performed using the spherical, exponential, and Gaussian models.

4.3. Cross-validation

The cross-validation procedure ignores an observation in the dataset, and uses the remaining observations to estimate the ignored observation using a particular interpolation technique. The process is repeated for each observation in the dataset to obtain a complete set of interpolated values by each technique. Validation should be carried out before producing the final surface, where it helps in making an informed decision as to which model provides the best predictions should have [28]. The best-fitted semi-variogram model parameters for the gas content data of the three coal seams are given in Table 4.

For a model that provides unbiased predictions, the mean prediction errors (MPEs) should be close to zero. Again, for a correct assessment of the variability, and to check if the prediction standard errors are appropriate and valid, the root-mean-square prediction error (RMSPE) and the average standard prediction error (ASE) should be similar, and the root-mean square standardized prediction error (RMSSPE) should be close to one [26, 29].

The results of cross-validation and also prediction error for each semi-variogram model selected for the C_1 and B_2 coal seams are shown in Figure 7 and Table 5. As shown in Figure 7, the differences between the measured and predicted data values are small, indicating a high accuracy level of the selected model.

Table 4. Best-fitted semi-variogram model parameters of coal seam gas contents.

Parameters / Coal seam	Model	Nugget effect	Lag size (m)	Number of Lag	Neighbors to include	Include at least	Large diameter of anisotropy ellipse (m)
C_1	Spherical	0.076	90	12	11	4	1066
C_2	Exponential	0	100	12	10	5	1185
B_2	Spherical	6.8	200	12	14	7	2331

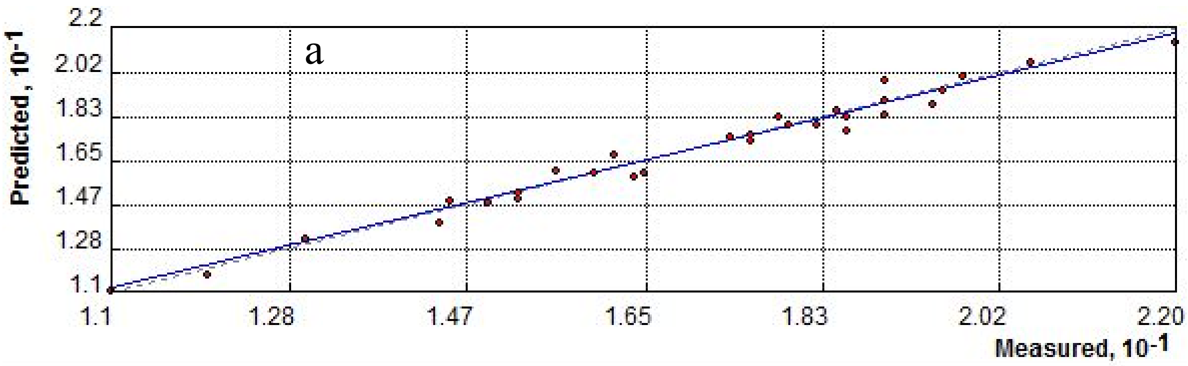

Regression Function: 0.960*X + 0.646

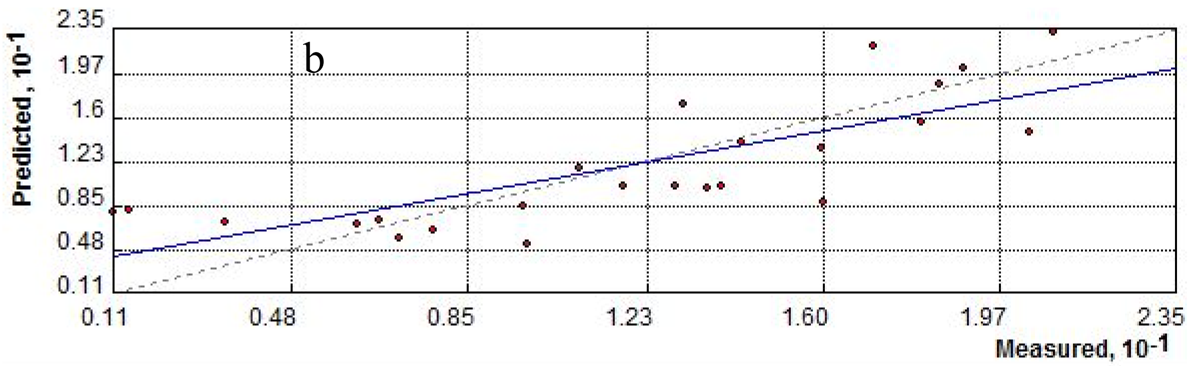

Regression Function: 0.715*X + 3.419

Figure 7. Cross-validation of the semi-variogram model for coal seams: a) C_1 and b) B_2 .

Table 5. Prediction errors from semi-variogram model.

Prediction error / Coal seam	Model	MPE	RMSPE	ASE	RMSSPE
C_1	Spherical	-0.003	0.393	0.390	1.023
C_2	Exponential	0.32	5.13	7.21	1.07
B_2	Spherical	-0.023	3.618	3.75	0.974

4.4. Prediction map

The final prediction map (i.e. continuous surface) of the three coal seam gas contents in Tabas coal mine was created in ArcGIS (Figure 8). As seen, about seven of nine panels designed in the C_1 coal seam have gas contents more than 15 m^3/ton. In other words, about 84% of the understudied area in the C_1 coal seam pertains to the over-class coal gas content group.

In order to prevent the high gas content-related problems in these panels, the use of a gas drainage system is suggested. Also the analysis results reveal that approximately 55% and 25% of the understudied area, respectively in the B_2 and C_2 coal seams, fall in the over-class category. As it can also be followed in Figure 8, for all the three coal seams, the gas content increases with the depth. Higher gas content values are observed in the deeper panels (i.e. E_3, E_4, E_5, W_3, and W_4). As it can be seen in the prediction map of C_2 in this figure, there is a small area at the end of the E1 panel showing a high gas content. This is due to the presence of a fault zone in this area, resulting in an increased coal gas content. A fault creates a fractured and low pressure region, resulting in a localized zone of high gas content.

Figure 9 shows the variation in the gas content data with respect to seam depth obtained from boreholes drilled in C_1. As it can be seen in Figure 9, the gas content increases directly with increase in the seam depth. Also, as followed in this figure, the gas content exceeds 15 m^3/ton when the depth of the coal seam reaches nearly 300 m. This is of critical importance to maintain the safety standards in the next remaining longwall panels that are deeper than 300 m.

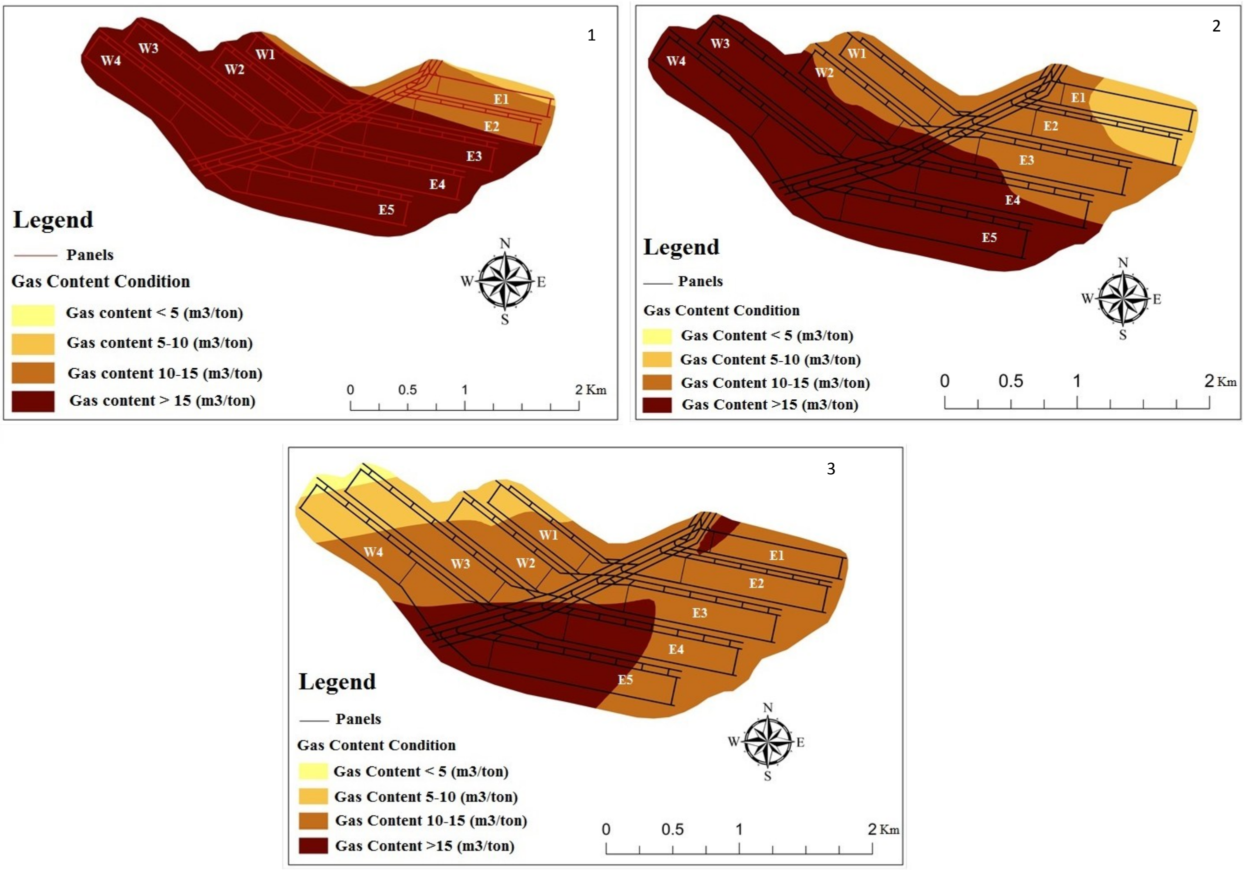

Figure 8. Gas content prediction map of three coal seams: 1) C_1 2) B_2, and 3) C_2.

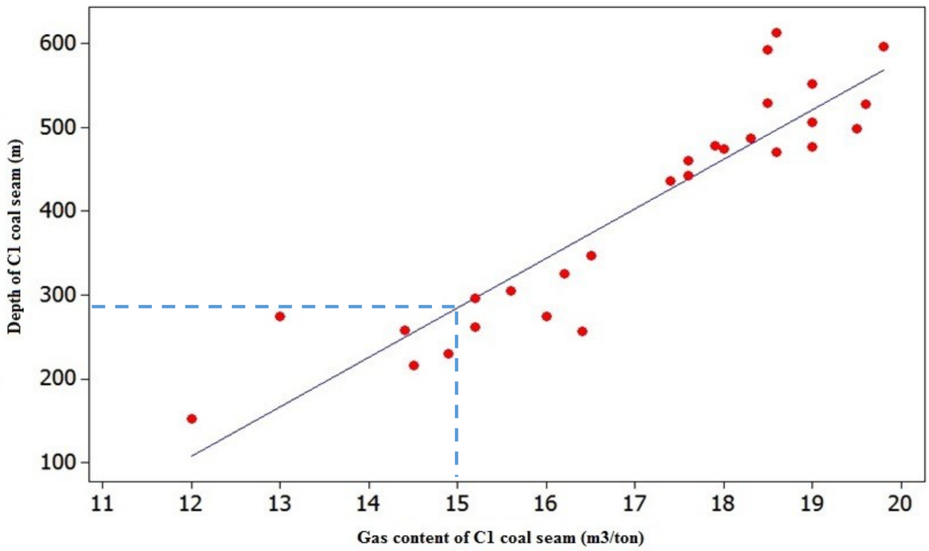

Figure 9. Relationship between C_1 seam gas content and depth data.

5. Conclusions

As a preliminary study to evaluate the gas drainage and CBM production potential, the gas contents of three coal seams (i.e. C_1, C_2, and B_2) in Tabas coal mine, Parvadeh#1, were estimated using the exploration drilling data and geostatistical analysis. The results obtained from the gas content prediction map of the C_1 coal seam showed that about 84% of the understudied area had a gas content more than 15 m^3/ton, pertaining to the over-class gas content group. Also about 55% of the B_2 coal seam had a gas content more than 15 m^3/ton. The high gas content of the B_2 coal seam is important in such a way that the methane gas released from the seam will penetrate into the under-extraction longwall panel or gob area of the C_1 coal seam, and accordingly, will result in a high gas concentration. The results obtained from a similar analysis on the gas content prediction map for the C_2 coal seam showed that about 25% of the understudied area had a gas content more than 15 m^3/ton.

Coal extraction leads to the formation of a low pressure region in C_1. According to the fact of gas movement from high to low present environments, the methane gas present in the adjacent coal seams (i.e. B_2 and C_2) tends to move towards the C_1 longwall stope and gob.

The mining depth is an important factor with respect to the coal seam gas content. With increase in the mining depth, the gas contents of the coal seams increase. Hence, in the next remaining panels, with mining depths deeper than 300 m, use of methane pre-drainage strategies to help mitigate expected gas emission problems should be taken into consideration.

References

[1]. Kim, A.G. (1977). Estimating Methane Content of Bituminous Coalbeds from Adsorption Data, U.S. Bureau of Mines Report of Investigations, RI8245.

[2]. Bochorishvili, N., Chikhradze, N., Mataradze, E., Akhvlediani, I., Chikhradze, M. and Krauthammer, T. (2015). New Suppression System of Methane Explosion in Coal Mines. Procedia Earth and Planetary Science. 15: 720-24.

[3]. Black, J. (2011). Factors Affecting the Drainage of Gas From Coal and Methods to Improve Drainage Effectiveness, Ph.D. Thesis, University Of Wollongong, School of Civil, Mining and Environmental Engineering.

[4]. Mohr, S.H. and Evans, G.M. (2009). Forecasting coal production until 2100. Fuel. 88: 2059-2067.

[5]. Darling, P. (2011). SME Mining Engineering Handbook. 3rd edition, SME.

[6]. Karacan, C.Ö. (2008). Modeling and prediction of ventilation methane emission of U.S. longwall mines using supervised artificial neural networks. International Journal of Coal Geolog. 73: 371-387.

[7]. Karacan, C.Ö., Olea, R. and Goodman, G. (2012). Geostatistical modeling of the gas emission zone and its in-place gas content for Pittsburgh-seam mines using sequential Gaussian simulation. International Journal of Coal Geology. 90: 50-71.

[8]. Chen, K.C., Irawan, S. and Sum, C.W. (2011). Preliminary study on gas storage capacity and gas-in-place for CBM potential in Balingian Coalfield, Sarawak Malaysia. International Journal of Applied Science and Technology. 1 (2): 82-94.

[9]. Lv, Y., Tang, D., Xu, H. and Luo, H. (2012). Production characteristics and the key factors in high-rank coalbed methane fields: A case study on the Fanzhuang Block, Southern Qinshui Basin, China. International Journal of Coal Geology. 96: 93-108.

[10]. Hu, X., Yang, S., Zhou, X., Zhang, G. and Xie, B. (2014). A quantification prediction model of coalbed methane content and its application in Pannan coalfield, Southwest China. Journal of Natural Gas Science and Engineering. 21: 900-906.

[11]. Fu, H., Tang, D., Xu, H., Xu, T., Chen, B., Hu, P., Yin, Z., Wu, P. and He, G. (2016). Geological characteristics and CBM exploration potential evaluation: A case study in the middle of the southern Junggar Basin, NW China. Journal of Natural Gas Science and Engineering. 30: 557-570.

[12]. Sarhosis, V., Jaya, A.A. and Thomas, H.R. (2016). Economic modelling for coal bed methane production and electricity generation from deep virgin coal seams. Energy. 107: 580-594.

[13]. Sereshki, F., Vaezian, A. and Saffari, A. (2016). Evaluation of effect of macerals on coal permeability in Tazareh and Parvadeh mines. J Stratigr Sedimentol Res. 63 (2): 1-22.

[14]. Taheri, A., Sereshki, F., Ardejani, F.D. and Mirzaghorbanali, A. (2017). Simulation of macerals effects on methane emission during gas drainage in coal mines. Fuel. 210: 659-665.

[15]. Ghanbari, K., Ataei, M., Sereshki, F. and Saffari, A. (2018). Determination and assessment of coal bed methane potential using rock engineering systems. Journal of Mining and Environment. DOI: 10.22044/jme.2018.6649.1486.

[16]. Prakash, A. and Vekerdy, Z. (2004). Design and implementation of a dedicated prototype GIS for coal fire investigations in North China. Int J Coal Geol. 59 (1-2): 107-119.

[17]. Johnson, N., Yang, C. and Ogden, J. (2008). A GIS-based assessment of coal-based hydrogen infrastructure deployment in the state of Ohio. International Journal of Hydrogen Energy. 33 (20): 5287-5303.

[18]. Şalap, S., Karslıoğlu, M.O. and Demirel, N. (2009). Development of a GIS-based monitoring and management system for underground coal mining safety. International Journal of Coal Geology. 80 (2): 105-112.

[19]. Yao, Y., Liu, D., Tang, D., Tang, S., Che, Y. and Huang, W. (2009). Preliminary evaluation of the coalbed methane production potential and its geological controls in the Weibei Coalfield, Southeastern Ordos Basin, China. Int J Coal Geol. 78 (1): 1-15.

[20]. Sutcu, E.C. (2012). Use of GIS to discover potential coalfields in Yatagan- Milas area in Turkey. International Journal of Coal Geology. 98: 95-109.

[21].Vaziri, V., Khademi Hamidi, J. and Sayadi, A.R. (2015). Estimation of coal gas content using geostatisti cal methods in GIS environment: a case study from Ta bas coal mine. In: Proceedings of the 24th international mining congress of Turkey IMCET. pp. 1007-1015.

[22]. Vaziri, V., Khademi Hamidi, J. and Sayadi, A.R. (2018). An integrated GIS-based approach for geohazards risk assessment in coal mines. Environmental Earth Sciences. 77 (1): 29.

[23].Margaret, A.
and Carignan, J. (1997). Géostatistiquelinéaire: applica tion au domaineminier. Les Presses de l'Ecole des Min es, Paris.

[24]. Oliver, M.A. and Webster, R. (1990). Kriging: a method of interpolation for geographical information systems. International Journal of Geographic Information System. 4 (3): 313-32.

[25]. Johnston, K., Ver Hoef, J.M., Krivoruchko, K. and Lucas, N. (2001). Using ArcGIS Geostatistical Analyst. Vol. 380, Redlands: Esri.

[26]. Kamble, K.H. and Aggrawal, P. (2011). Geostatistical Analyst for Deciding Optimal Interpolation Strategies for Delineating Compact Zones. International Journal of Geosciences. 2 (4): 585-596.

[27]. Olea, R.A. (2006). A six-step practical approach to semivariogram modeling. Stochastic Environmental Research and Risk Assessment. 20 (5): 307-318.

[28]. McCoy, J. and Johnston, K. (2001). Using ArcGIS Spatial Analyst: GIS by ESRI. Environmental Systems Research Institute.

[29]. Burke, S., Chu, G., Heyer, J., Lee, J., Tang, X., Tran, T. and Zhang, L. (2013). Mass Quantification of PCE in Los Angeles Groundwater from the GeoTracker Database, Los Angeles, UCLA Institute of the Environment and Sustainability Senior Practicum, Los Angeles, CA.

تخمین گازخیزی لایه‌های زغال‌سنگ به منظور ارزیابی پتانسیل استفاده از سیستم‌های زهکشی گاز متان در معدن زغال‌سنگ طبس

موبد محتشم سیفی[۱]، جعفر خادمی حمیدی[۱*]، مسعود منجزی[۱] و علی حسینی[۲]

۱- بخش مهندسی معدن، دانشکده فنی و مهندسی، دانشگاه تربیت مدرس تهران، ایران
۲- شرکت زغال‌سنگ پروده طبس، ایران

ارسال ۲۰۱۸/۲/۱۲، پذیرش ۲۰۱۸/۳/۱۸

* نویسنده مسئول مکاتبات: jafarkhademi@modares.ac.ir

چکیده:

انتشار، تجمع و انفجار گاز متان، مهم‌ترین عامل ایجاد خطر در معادن زیرزمینی زغال‌سنگ است؛ از این‌رو، اطلاع از گازخیزی لایه‌های زغالی در معادن زیرزمینی زغال‌سنگ، به منظور جلوگیری از خطر انفجار، حفظ ایمنی معدن کاران و جلوگیری از خسارات جانی و مالی، بسیار حائز اهمیت است. هدف از پژوهش حاضر، پهنه‌بندی گازخیزی لایه‌های زغال‌سنگ C_1، C_2 و B_2 و نیز شناسایی پهنه‌های با گازخیزی زیاد در معدن زغال‌سنگ شماره ۱ پروده طبس، بر اساس داده‌های به دست آمده از گمانه‌های اکتشافی است. به منظور تخمین میزان گازخیزی لایه‌های زغال‌سنگ معدن طبس در نقاط فاقد داده، از ابزار تخمینگر زمین‌آماری کریجینگ در محیط نرم‌افزار سیستم اطلاعات جغرافیایی Arc GIS استفاده شد. بررسی نقشه‌های گازخیزی نشان داد که حدود ۸۴ درصد از لایه زغال‌سنگ C_1، ۵۵ درصد از لایه زغال‌سنگ B_2 و ۲۲ درصد از لایه زغال‌سنگ C_2 در منطقه مورد مطالعه، دارای گازخیزی بیش از ۱۵ مترمکعب بر تن است. نتایج این پژوهش، ضرورت استفاده از سیستم‌های پیش‌زهکشی به ویژه در هنگام معدنکاری پهنه‌های عمیق‌تر را به خوبی نشان می‌دهد.

کلمات کلیدی: گازخیزی، سیستم اطلاعات جغرافیایی، زمین‌آمار، نقشه پیش‌بینی.